Protein Science (1999), *8*:2270–2280. Cambridge University Press. Printed in the USA.

The solution structure of the anti-HIV chemokine vMIP-II

ANDY C. LIWANG,[1] ZI-XUAN WANG,[2] YI SUN,[2] STEPHEN C. PEIPER,[2]
AND PATRICIA J. LIWANG[3,4]

[1]Texas A&M University, Department of Biochemistry and Biophysics, College Station, Texas 77843-2128
[2]James Graham Brown Cancer Center, University of Louisville, Louisville, Kentucky 40202
[3]Purdue University, Department of Chemistry, West Lafayette, Indiana 47907

(RECEIVED March 17, 1999; ACCEPTED July 23, 1999)

Abstract

We report the solution structure of the chemotactic cytokine (chemokine) vMIP-II. This protein has unique biological activities in that it blocks infection by several different human immunodeficiency virus type 1 (HIV-1) strains. This occurs because vMIP-II binds to a wide range of chemokine receptors, some of which are used by HIV to gain cell entry. vMIP-II is a monomeric protein, unlike most members of the chemokine family, and its structure consists of a disordered N-terminus, followed by a helical turn (Gln25–Leu27), which leads into the first strand of a three-stranded antiparallel β-sheet (Ser29–Thr34; Gly42–Thr47; Gln52–Asp56). Following the sheet is a C-terminal α-helix, which extends from residue Asp60 until Gln68. The final five residues beyond the C-terminal helix (Pro70–Arg74) are in an extended conformation, but several of these C-terminal residues contact the first β-strand. The structure of vMIP-II is compared to other chemokines that also block infection by HIV-1, and the structural basis of its lack of ability to form a dimer is discussed.

Keywords: chemokine; KSHV; NMR; structure; vMIP

*Chemo*attractant cyto*kines*, chemokines, are products of the largest family of cytokine genes, numbering over 40, that encode secreted proteins of 8–12 kDa (Oppenheim et al., 1991; Schall, 1991; Baggiolini et al., 1997). Chemokines promote inflammation by inducing the directed migration of leukocytes, and they are distinguished by their specificity for subsets of leukocytes (Baggiolini, 1998). Additional roles include the modulation (both positive and negative) of angiogenesis and growth regulatory functions (Rollins, 1997). The family is recognized by the presence of four positionally conserved cysteine residues, although there is also similarity at the level of primary structure. It is divided into four branches, or subfamilies, based on the configuration of the two amino-proximal cysteine residues. The two main branches are CXC, in which the N-terminal cysteine residues are separated by a single residue, and CC, in which these cysteines are juxtaposed (Baggiolini et al., 1997). In addition, there are two exceptions, each of which could be considered a separate branch. Lymphotactin has two cysteine residues with only one in the amino-proximal location (-C- branch) (Kelner et al., 1994) and neurotactin/fractalkine has a C-X3-C chemokine module that is expressed on the cell surface via a mucinous stalk (Bazan et al., 1997). The majority of the genes encoding CXC and CC chemokines are located in gene clusters on chromosomes 4q13 and 17q11.2-12, respectively, and share a common exon–intron structure (CXC, 4 exons; CC, 3 exons) (Baggiolini et al., 1997).

Receptors that mediate the cellular effects of chemokines are members of the serpentine receptor superfamily that have seven hydrophobic helices and are coupled to heterotrimeric G-proteins for signal transduction. Chemokine receptors may be specific for one ligand, but are typically shared in that they bind several chemokines within the same subfamily (Holmes et al., 1991; Murphy & Tiffany, 1991; Neote et al., 1993; Samson et al., 1996). The single exception to this rule is the Duffy chemokine receptor, which binds to selected members of the CXC and CC branches, but has not been shown to transduce a signal (Hadley & Peiper, 1997). In addition to their role in normal pathophysiology, a subset of chemokine receptors has been implicated as portals of entry for infectious agents. The initial example was the Duffy chemokine receptor, which was shown to be necessary for the invasion of erythroid

Reprint requests to: Patricia J. LiWang, Department of Biochemistry and Biophysics, Texas A&M University, College Station, Texas 77843-2128; e-mail: pliwang@bioch.tamu.edu (and correspondence regarding the structure); or Stephen C. Peiper, James Graham Brown Cancer Center, University of Louisville, Louisville, Kentucky 40202; e-mail: scp@bcc.louisville.edu (and correspondence regarding the vMIP-II construct).

[4]Present address: Texas A&M University, Department of Biochemistry and Biophysics, College Station, Texas 77843-2128.

Abbreviations: CC chemokines: MIP-1β; macrophage inflammatory protein-1β; MIP-1α, macrophage inflammatory protein-1α; MCP, monocyte chemoattractant protein; RANTES, regulated on activation of normal T-cell expressed and secreted; *CXC chemokines*: IL-8, interleukin-8; MGSA, melanoma growth-stimulatory activity; NAP-2, neutrophil-activating peptide-2; PF-4, platelet factor-4; NMR, nuclear magnetic resonance; HSQC, heteronuclear single quantum coherence; HMQC, heteronuclear multiple quantum coherence; rf, radio frequency; DSS, 2,2-dimethyl-2-silapentane-5-sulfonate, sodium salt; EDTA, ethylenediamine tetraacetic acid; NOE, nuclear Overhauser effect; NOESY, NOE spectroscopy.

cells by *Plasmodium vivax* (Hadley & Peiper, 1997). However, the finding that a cadre of chemokine receptors functioned as coreceptors for entry of the human immunodeficiency virus type 1 (HIV-1) by ENV-mediated fusion sparked intense interest in this paradigm (Alkhatib et al., 1996; Bleul et al., 1996; Deng et al., 1996; Dragic et al., 1996; Oberlin et al., 1996; Doms & Peiper, 1997). Because the binding of cognate ligands (the chemokines) to coreceptors blocks HIV-1 infection at the stage of viral entry, the structural basis for the specificity of receptor engagement has come under intense investigation. Attempts to develop coreceptor antagonists have been complicated by the multiplicity of chemokine receptors that can be utilized in ENV-mediated fusion, which, in effect, results in a "moving molecular target" that may require agents that have a broad specificity for a wide range of chemokine receptors.

The discovery and sequencing of the Kaposi's sarcoma-associated herpesvirus led to the identification of two open reading frames that were predicted to encode proteins with features of chemokines. Both encode CC chemokines with homology to MIP-1α and MIP-1β (Moore et al., 1996). Characterization of the recombinant proteins revealed that one, designated vMIP-II, showed promiscuous binding to receptors, including receptors for CC and CXC chemokines (Boshoff et al., 1997; Kledal et al., 1997). The repertoire included three coreceptors thought to be most relevant to the pathogenesis of HIV-1 infection, CCR5, CCR3, and CXCR4 (Boshoff et al., 1997; Kledal et al., 1997). Whereas vMIP-II has been shown to be an agonist for CCR3, it is an antagonist of the remaining (co)receptors that it binds, including CCR5 and CXCR4 (Boshoff et al., 1997; Kledal et al., 1997; Sozzani et al., 1998). Understanding of the structural basis for the uniquely unrestricted receptor binding repertoire of vMIP-II may provide insight into requirements for chemokine receptor binding that will empower the design of broadly active coreceptor antagonists.

The structures of several CC chemokines have been determined previously (Clore et al., 1990; Kim et al., 1994, 1996; Lodi et al., 1994; Zhang et al., 1994; Chung et al., 1995; Skelton et al., 1995; Handel & Domaille, 1996; Meunier et al., 1997; Dealwis et al., 1998), and provide a wealth of data for comparisons of structure–activity relationships. Although each member of this subfamily has a consistent "chemokine fold" that is comprised of a series of three antiparallel β-strands followed by a C-terminal α-helix, there are important differences between members of this family in at least two areas. First, although chemokines share a significant degree of similarity of amino acid residues in their regions of common secondary structure, the N-terminus of each chemokine is largely distinct in sequence from the others, even among members of the same subfamily (Schall, 1991). The N-terminus has been implicated in chemokine function, as it has been shown that truncation or mutation in this region can lead to a dramatic change in activity. For instance, truncation at the N-terminus can result in the loss of agonist activity and the gain of potent antagonist function (Moser et al., 1993; Gong & Clark-Lewis, 1995; Gong et al., 1996; Crump et al., 1997). In the CC chemokine RANTES, changes of individual amino acids at the N-terminus can specify loss of binding ability or activating ability to one (but not all) of the receptors utilized by the chemokine (Pakianathan et al., 1997). In addition, the deletion of a single N-terminal amino acid from the CC chemokine MCP-1 sharply reduced its activity on basophil leukocytes. This slight alteration in protein sequence also imparted upon the chemokine the ability to activate eosinophils, an activity likely mediated by a separate receptor (Weber et al., 1996). It has also been shown that addition to the N-terminus of RANTES produced a potent antagonist (Wells et al., 1996; Simmons et al., 1997), while adding to the N-terminus of the CXC chemokine SDF-1 increased the activity of the protein (Crump et al., 1997).

A region within the N-terminus has been termed the "N-loop" and includes the amino acids immediately after the conserved cysteines (Fig. 1). This region, although not part of a typical secondary structural motif, is structurally much better defined than the more N-terminal amino acids, and has been postulated to also play a role in the chemokines' diverse interactions with their receptors (Clark-Lewis et al., 1995; Schraufstatter et al., 1995; Pakianathan et al., 1997). The N-loop of chemokines also has significant sequence variation, which may affect both the activity and the structure of these proteins.

The second major difference among chemokines is their disparate quaternary structure. Most structures of chemokines reveal a protein dimer (Clore et al., 1990; Fairbrother et al., 1994; Kim et al., 1994; Lodi et al., 1994; Chung et al., 1995; Skelton et al., 1995; Handel & Domaille, 1996; Meunier et al., 1997; Dealwis et al., 1998; Hanzawa et al., 1998; Shao et al., 1998b), with some showing higher order multimers (Zhang et al., 1994; Mayo et al., 1995). Interestingly, the structural form of the dimer of CC chemokines (such as MIP-1β) is distinct from that of the CXC chemokines. The dimer interface of the CC chemokine is located at the N-terminus of the protein and is centered near the conserved cysteines, involving many amino acids that have been implicated in receptor binding. In contrast, the CXC chemokine dimers are formed by the antiparallel positioning of strand β1, resulting in a completely different overall shape and the subsequent exposure of surface residues different than in the CC subfamily (see, for example, Clore et al., 1990; Kim et al., 1994; Lodi et al., 1994; Handel & Domaille, 1996). This difference in dimer structure is unique and interesting from a structural standpoint and also may contribute to the distinct set of activities for each subfamily. Alternatively, the differing protein–protein interactions of each dimer may mimic the binding of the chemokine to the receptor surface,

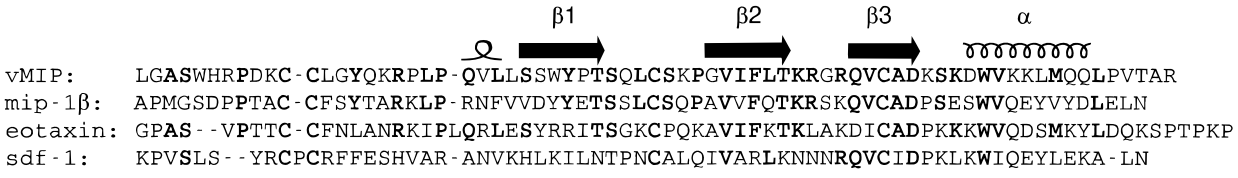

Fig. 1. Pairwise amino acid sequence alignments of vMIP-II with MIP-1β, eotaxin, and SDF-1 using the program CLUSTALW (Thompson et al., 1994). Amino acids shown in bold are identical to vMIP-II at that position. The present work utilizes the mature N-terminus of vMIP-II, which in our numbering system begins at residue Leu4. Also shown are the positions of the secondary structural units for vMIP-II.

providing part of the explanation for the lack of cross-binding between the chemokines of one subfamily and the receptors of the other subfamily.

The physiological significance of chemokine self-association (dimerization) has not been elucidated. It has been established that the formation of a chemo-attractant gradient is essential to the induction of directed migration of leukocytes, and it has been postulated that this may be developed through the association of chemokines with proteoglycans (Tanaka et al., 1993; Wagner et al., 1998). The role of the dimer in chemokine activity is controversial, as some chemokines have been shown to be active when modified to exclude the possibility of dimer formation (Rajarathnam et al., 1994, 1997; Paavola et al., 1998). In addition, some recent chemokine structures have reported monomeric structures (Kim et al., 1996; Crump et al., 1997, 1998), although in each case it appears that solution conditions could be altered to produce either a monomer or a dimer form.[5] However, there is also evidence that obligate chemokine dimers are active (Zhang & Rollins, 1995; Leong et al., 1997), and recent work has shown that cell surface sugars act to locally concentrate chemokines, suggesting that chemokines may be multimeric in the microenvironment of the cell surface (Hoogewerf et al., 1997). The wide variety of activity of chemokines and their importance in human health make a study of the structural features of chemokines that lead to each activity essential.

We report the solution structure of vMIP-II. We and others have shown that vMIP-II is fully a monomer in solution, even at high concentrations (LiWang et al., 1999; Shao et al., 1998a) and, unlike most or all other chemokines, this protein appears to have no tendency to dimerize under conditions of altered salt or pH. Not only is this steadfast monomer interesting from a structural standpoint, the lack of dimerization may bear upon the ability of vMIP-II to bind a wide variety of chemokine receptors, including CCR1, CCR2, CCR3, CCR5, and even the CXCR4 receptor of the other chemokine subfamily (Boshoff et al., 1997; Kledal et al., 1997). We discuss the structural features that are likely to contribute to maintaining the monomeric form of vMIP-II and compare the structure of this protein to several other chemokines, each possessing a facet of the broad receptor binding ability of vMIP-II.

Results

Description of the structure

A family of 30 structures of vMIP-II was calculated, based on numerous interproton distance and angle restraints, and is shown in Figure 2A. To be consistent with the reported mature form of vMIP-II (Kledal et al., 1997), the present work was carried out on a protein having a shorter N-terminus than the protein used in our previous vMIP-II dynamics publication (LiWang et al., 1999). The vMIP-II used for the present work begins with amino acid Leu4 using our numbering system. In addition, the pH of the sample in our previous work (LiWang et al., 1999) was 2.5, for maximum solubility and for consistency with the similar protein MIP-1β (Lodi et al., 1994). In the present work, we opted for a pH value closer to neutrality (pH 5.4), which produced nearly identical resonance assignments as the previous sample,[6] but a decrease in sample solubility.

To confirm that the present sample is composed entirely of a monomeric protein, we performed ^{15}N T_1 and T_2 relaxation experiments similar to those in our dynamics study (LiWang et al., 1999). It has been well established that ^{15}N relaxation parameters are strongly dependent on the size of a protein (Kay et al., 1989; Farrow et al., 1994; Laurence et al., 1998), and experiments to determine these parameters have been carried out on several chemokines (Grasberger et al., 1993; Laurence et al., 1998; LiWang et al., 1999). The data for the present vMIP-II protein at pH 5.4 reveal an overall correlation time of 4.2 $\pm$ 0.3 ns, which is consistent with a monomeric protein of 71 amino acids. For the vMIP-II (containing an extended N-terminus) that we used in our dynamics calculations, the data showed a correlation time of 4.7 $\pm$ 0.3 ns for 77 amino acids, again revealing a monomer (LiWang et al., 1999). The difference in the two correlation time values is consistent with the difference in molecular weight of the two proteins. These values for vMIP-II are also wholly consistent with other work showing a mutant MIP-1β monomer with a correlation time of 4.5 ns (Laurence et al., 1998). In addition, others have used diffusion measurements at pH 3.25 to demonstrate that synthesized vMIP-II is a monomer (Shao et al., 1998a).

The root-mean-square deviation (RMSD) of the 30 structures from the minimized mean structure is 0.31 Å for the backbone N, C$^{\alpha}$, and C$'$ over residues 14 to 72. For the same residues the RMSD for all heavy atoms (excluding hydrogens) is 0.77 Å. As noted in Table 1, the family of structures was calculated from 946 nontrivial NOE restraints (that is, excluding vicinal NOE peaks when a stereoassignment was not possible), 27 χ1 angle restraints, and three χ2 angle restraints (for Leu28, Leu65, and Leu69). The program X-PLOR was used for the calculations, using the distance geometry/simulated annealing protocols of Nilges et al. (Nilges et al., 1988, 1991; Kuszewski et al., 1992). Twenty-eight backbone hydrogen bonding restraints were determined based on slow amide exchange with solvent (LiWang et al., 1999) and were added at the later stages of refinement. The backbone hydrogen bonds were also supported by NOE cross peaks between nearby protons and by consistently close distances in the calculated families of structures. Fifty-five $^{3}J_{\mathrm{HNH}\alpha}$ coupling constant restraints were also used to restrain ϕ angles (Lodi et al., 1994). Therefore, in total, the structure of vMIP-II was calculated with 18.1 restraints per residue in the region Cys14–Thr72, 14.9 restraints per residue for the whole protein.

As noted previously (LiWang et al., 1999) the N-terminal 13 amino acids (Gly4–Lys16) and the C-terminal two amino acids of

[5] SDF-1: Crump et al. (1997) carefully document the lack of a dimer for SDF-1 under some solution conditions but Dealwis et al. (1998) report that an active variant of SDF-1 is a dimer in the crystal structure. MCP-3: Two groups have reported the solution structure of this protein, one deducing that the protein is a monomer (Kim et al., 1996), the other seeing evidence of a dimer (Meunier et al., 1997). Eotaxin: Crump et al. (1998) discuss adjusting solution conditions to favor the monomer form of the protein over the dimer form.

[6] A chemical shift comparison of both recombinant proteins reveals very few differences except in the very N-terminal region (the vMIP-II from our previous paper began with AMAGDTLGA . . . , while the vMIP-II in the present work simply begins with LGA . . .). Although Leu4 at the N-terminus is unobserved in the present protein, only the next four amide protons, and Arg51 and Lys63 show changes greater than 0.03 ppm (0.37, 0.23, 0.06, 0.17, 0.04, and 0.05 ppm, respectively). In addition, only Gly5 and Ser7 show a ^{15}N chemical shift changes greater than 0.75 ppm when compared to the old construct, and indeed, there are no ^{15}N chemical shift changes greater than 0.2 past position Asp12. This comparison was carried out at similar pH values for both constructs (pH 5). In our previous comparison of pH 2.5 vs. pH 5 vMIP-II from the older construct, we also showed very few chemical shift changes except in a few charged residues (LiWang et al., 1999).

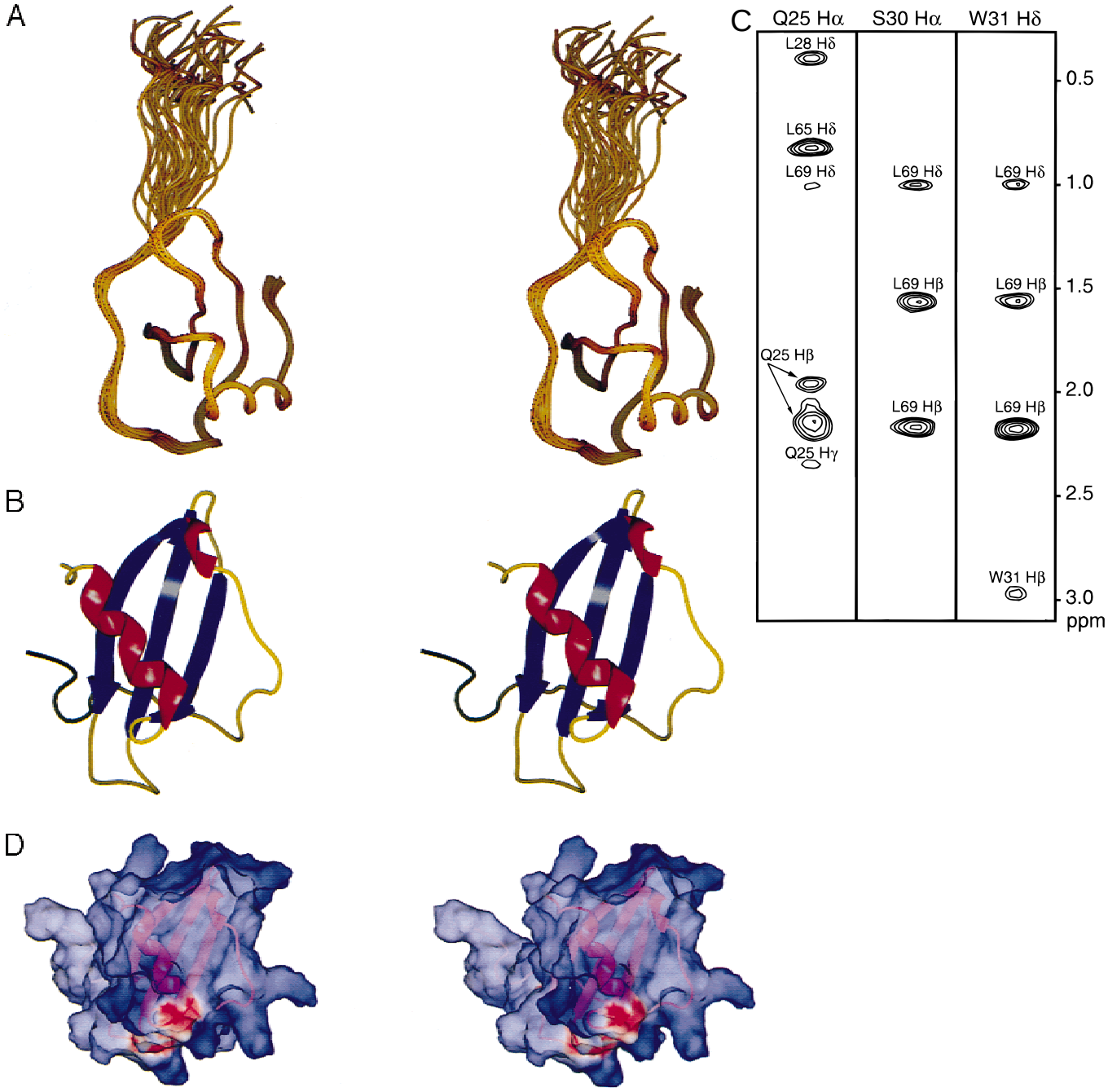

Fig. 2. A: A stereoview of the overlay of the family of 30 structures of vMIP-II (superimposed with best fit to Cα) from residues 14–72. **B:** A stereoview of the ribbon diagram of vMIP-II. **C:** Three regions from the ^{13}C NOESY data, showing long-range connections between amino acids near the first β-strand and amino acids near the C-terminus. **D:** A surface of vMIP-II showing electrostatic potential, calculated by the program SPOCK. Blue shows positively charged areas, while red shows negatively charged areas. Visible underneath the surface is a ribbon drawing of the protein. Figures 2A, 2B, and 2D were created using the program SPOCK (Christopher, 1998).

vMIP-II undergo significant internal motion. The structure of vMIP-II, shown in Figures 2A and 2B, consists of a disordered N-terminal region having a substantial number of sequential NOE contacts beginning at residue Trp8, but having no long-range NOE contacts until Cys14, with these due largely to the participation of both Cys14 and Cys15 in disulfide bonds (to Cys38 and Cys54, respectively). A helical turn from residues Gln25 to Leu27 leads into the first of three β-strands, beginning at residue Ser29. Strand β1 extends from residues Ser29 to Thr34 and includes a proline at position 33 (unusual for a β strand; Minor & Kim, 1994). The ϕ angle of each proline (including Pro33) was constrained in later stages of refinement and without violation to range from -53 to $-73°$ (MacArthur & Thornton, 1991), and the structure reveals a ψ angle of 137° for Pro33, largely consistent with the canonical

Table 1. *Structural statistics for vMIP-II for 30 final structures*[a]

Distance restraints	
Intraresidue ($i - j = 0$)	320
Sequential ($\|i - j\| = 1$)	246
Medium range ($\|i - j\| = 4$)	127
Long range ($\|i - j\| > 4$)	253
Total distance restraints	946
Dihedral angle constraints, χ (27 χ1, 3 χ2)	30
$^3J_{HNH\alpha}$ coupling constants (Vuister & Bax, 1993; Kuboniwa et al., 1994)	55
Hydrogen bonds (two restraints per 28 H-bonds)	28
Mean RMSDs from experimental restraints[b]	
Distance (Å)	0.067 ± 0.001
Dihedral angle (deg)	0.4 ± 0.1
RMSD from $^3J_{HNH\alpha}$ coupling constants (Hz)	0.22 ± 0.01
Deviations from idealized covalent geometry	
Bonds (Å)	0.0032 ± 0.0001
Angles (deg)	0.50 ± 0.02
Impropers (deg)	0.53 ± 0.02
PROCHECK Ramachandran analysis (Laskowski et al., 1993)	
Most favored regions	86.8%
Additional allowed regions	12.8%
Generously allowed regions	0.2%
Disallowed regions	0.2%
Atomic RMSDs from the mean, minimized structure (Å)[3]	
Backbone (N,C$^\alpha$,C′) residues 14–72	0.31
Nonhydrogen residues 14–72	0.76

[a]The force constants used in the target function for simulated annealing are: 1,000 kcal mol^{-1} Å^{-2} for bond lengths, 500 kcal mol^{-1} rad^{-2} for angles and improper torsions, 4 kcal mol^{-1} Å^{-4} for quartic van der Waals repulsion, 50 kcal mol^{-1} Å^{-2} for experimental interproton distances and hydrogen bonds, 200 kcal mol^{-1} rad^{-2} for the torsion angle restraints, 10 kcal mol^{-1} Hz^{-2} for the $^3J_{HNH\alpha}$ coupling constant restraints, and 0.5 for the conformational database potential.

[b]None of the structures in the family exhibited NOE violations greater than 0.4 Å, and only three violations were above 0.3 Å. No dihedral restraints were violated by 2° or greater. No $^3J_{HNH\alpha}$ violations larger than 1.4 Hz were observed. Backbone hydrogen bonding restraints (two per hydrogen bond, $r_{N\text{-}O}$ = 2.4–3.5 Å, $r_{NH\text{-}O}$ = 1.5–2.8 Å) were deduced from slowly exchanging amide resonances and were added in the later stages of refinement. NOE distance restraints from protons on adjacent carbons were not used except in the case of H$^\alpha$ to stereoassigned H$^\beta$ protons.

[c]A total of 1,059 experimental restraints were used in the structure calculation, including 6 ϕ restraints [one for each proline (MacArthur & Thornton, 1991)], giving 14.9 restraints per residue for the whole protein (18.1 restraints per residue for residues 14–72).

β-strand geometry of around −100° for ϕ and +130° for ψ. An irregular turn follows the first β-strand, and leads into the β2 strand, which extends from residues 42 to 47 and shows numerous NOE contacts to both the β1 and β3 strands, fully consistent with an antiparallel β-sheet arrangement. The β3 strand extends from position Gln52 to Asp56 and leads into the C-terminal α-helix of vMIP-II, which extends from residue Asp60 to Gln68. The helix lies at about a 60° angle with respect to the β strands and is terminated shortly before the proline at position 70, after which the protein makes several long-range contacts with the β1 strand, as also shown in Figure 2C.

The family of structures, as well as the averaged, minimized structure, show a possible side-chain H-bond between the C-terminus of the protein and the β1 strand, which could explain why several residues beyond the C-terminal helix show moderately high-order parameters despite not being involved in a canonical secondary structural unit (LiWang et al., 1999). This putative H-bond is between the Ser30 side chain and the Thr72 side chain, with an average distance of 2.9 Å (HG to OG) in the family of structures, which is longer than generally accepted. There is also present a slightly more distant interaction between the Thr72 side chain and the Tyr32 backbone nitrogen. An additional H-bond occurs between the side chain of residue Thr47 and the backbone H^N of Arg51 (2.2 Å average distance between H^N and OG), which serves to stabilize the turn between the β2 and β3 strands. H-bonds are also consistently observed between the side chain of Ser35 and the H^N of Leu37 (2.4 Å average distance), and between the side chain of Asp56 and the H^N of Ser58 (2.7 Å average distance). Each of these H-bonds were inferred from interatomic distances that occur in both the minimized structure and are overwhelmingly present in the family of structures. These putative hydrogen bonds were not used as restraints in the structure calculations.

The side chains of the residues comprising the helix make many hydrophobic contacts with the β-sheet, including contacts between Met66 and both Trp31 and Val43 and between Leu65 and Phe45. The hydrophobic core of vMIP-II is approximately centered around the side chain of Phe45 and includes the side chains of Leu23, Leu28, Trp31, Val43, Phe45, Val53, Ala55, Trp61, Val62, Leu65, Met66, and Leu69. These findings are quite similar to those for the CC chemokine MIP-1β (Lodi et al., 1994) and are consistent with the general chemokine fold. Tyr18 and Ile44 are also significantly buried residues, although they are not located as part of the "core" of the protein.

The surface of vMIP-II is shown in Figure 2D and is similar in shape and charge distribution to the monomeric unit of MIP-1β (data not shown), with the most significant charge differences located on the loop leading to the C-terminal helix (where vMIP-II has more positive charge), and the region near the β1-strand (where vMIP-II lacks the negative charge of Asp30 MIP-1β). vMIP-II has two disulfide bonds, which can be categorized using bond angles by the method of Richards (Richardson, 1981). Accordingly, both the Cys14–Cys38 disulfide bridge and the Cys15–Cys54 disulfide are more consistent with the left-handed spiral conformation than with the right-handed hook.

We have previously investigated the backbone dynamics of vMIP-II (LiWang et al., 1999), and the present structure is consistent with our previous assumptions. As expected, the most ordered residues fall largely within regions of defined secondary structure, while the intervening loops between β-strands are less ordered. The N-terminal amino acids and those at the very C-terminus are the most disordered, as revealed both by our previous dynamics study, and consistent with our present structure determination.

Discussion

Here we report the high resolution structure of vMIP-II, a virally encoded CC chemokine that binds a unique repertoire of receptors, including CCR1 and CCR5, which engage the structurally related ligands MIP-1α and MIP-1β, as well as those that bind divergent chemokine ligands (i.e., CCR2b, MCP-1; CCR3, eotaxin and MCP-3; CCR8, I-309, and CXCR4, SDF-1) (Boshoff et al., 1997; Kledal et al., 1997). vMIP-II has a characteristic chemokine fold and contains a free amino terminus

that is followed by three antiparallel β-sheets and a carboxy-terminal α-helix, typical of other chemokines that have been analyzed. A structural model for the engagement and activation of the cognate receptor(s) by chemokines has been proposed in which distinct epitopes in the N-terminus proximal to the first β-sheet are responsible for these interactions (Clark-Lewis et al., 1995). It has been elegantly shown for RANTES that the precise residues that participate in binding and activation of signal transduction differ for different receptors (Pakianathan et al., 1997). The structural role of the scaffold of antiparallel β-sheets and the α-helix are critical to the activity of this N-terminal domain, as has been demonstrated for SDF-1, although a heterologous scaffold from IP-10 could also support the ability of the SDF-1 N-terminus to bind CXCR4 (Crump et al., 1997). The low identity between vMIP-II and the cognate ligands for the receptors that it can associate with raises the possibility that vMIP-II may employ a novel mechanism for high-affinity binding to chemokine receptors.

vMIP-II is a monomer

The high resolution analysis of vMIP-II structure as well as ^{15}N T_1 and T_2 relaxation data at pH 5.4 confirms previous findings that this viral chemokine does not self-associate (LiWang et al., 1999; Shao et al., 1998a). This lack of oligomerization, even at concentrations in the range of 1 mM, distinguishes vMIP-II from most other known chemokines, which have been shown to form dimers or multimers under various conditions (Clore et al., 1990; Fairbrother et al., 1994; Kim et al., 1994; Lodi et al., 1994; Zhang et al., 1994; Chung et al., 1995; Mayo et al., 1995; Skelton et al., 1995; Handel & Domaille, 1996; Meunier et al., 1997; Dealwis et al., 1998; Hanzawa et al., 1998; Shao et al., 1998b). The closely related human chemokine MIP-1β dimerizes through apposition of segments of the amino terminal domain in the region of the first canonical Cys residue (Lodi et al., 1994), a region that has low amino acid sequence identity with vMIP-II, suggesting a possible reason for the lack of an effective dimer interface in vMIP-II (vide infra).

Despite the importance from a structural standpoint of understanding the wide range of dimerization ability among the chemokines, our understanding of the significance of chemokine dimerization is, at best, incomplete. Many chemokines have been found to self-associate into homodimers at concentrations and conditions used for high resolution structural studies. It is clear that self-association is not required for biological activity for at least some chemokines, as variants that form obligate monomers bind ligand and induce signal transduction, as do those that constrain dimerization (Rajarathnam et al., 1994, 1997; Zhang & Rollins, 1995; Leong et al., 1997; Paavola et al., 1998). In addition, the dimer dissociation constant of several chemokines appears to be much higher than their physiological concentrations (Burrows et al., 1994; Paolini et al., 1994; Paavola et al., 1998). The monomer–dimer controversy is well illustrated by the apparently contradictory findings for MCP-1. Whereas in one report an N-terminally truncated MCP-1 formed heterodimers with wild-type MCP-1 and functioned as a dominant negative inhibitor of the wild-type protein (but could not interfere with chemically cross-linked dimers) (Zhang & Rollins, 1995), it was recently described by Paavola et al. (1998) that at least one point mutation in the N-terminus of this chemokine abrogates dimer formation, but does not alter receptor engagement and signaling.

Several chemokines have been reported to exist as monomers, even at high concentrations. These include MCP-3 (Kim et al., 1996), eotaxin (Crump et al., 1998), SDF-1 (Crump et al., 1997), fractalkine (Mizoue et al., 1999), and I-309 (Paolini et al., 1994). A conflicting report suggested that the CC chemokine MCP-3 formed a CXC-type homodimer (Meunier et al., 1997). Also, whereas one detailed analysis of SDF-1 failed to show evidence of dimerization (Crump et al., 1997), a crystallographic study showed a dimer interface typical of other CXC chemokines (Dealwis et al., 1998). NMR examination has revealed that eotaxin, which, like MCP-3, binds CCR3, exists in solution predominantly as a monomer, but that there is an equilibrium between monomeric and dimeric forms under some conditions (Crump et al., 1998). In our hands vMIP-II exists exclusively as a monomer, and preliminarily we have not found conditions that allow a detectable dimer form to exist in equilibrium with the monomer form.

Although vMIP-II induces signal transduction via CCR3, it has little homology in the N-terminal region (the site of dimer interface in other CC chemokines) with eotaxin, the primary ligand for this receptor, and with MCP-3. However, it appears that these three chemokines all exist preferentially as monomers in solution under the conditions used for NMR analysis. Our previous studies demonstrated that the N-terminal domain of vMIP-II is highly flexible and mobile, and structural studies on eotaxin show similar disorder in this region (Crump et al., 1998). In contrast, in CC chemokines that have a strong predilection to self-associate, the region at the N-terminal dimer interface is typically more structured (Chung et al., 1995; Skelton et al., 1995; Handel & Domaille, 1996). In addition, the available evidence suggests that the chemokine I-309 also exists as a monomer in solution (Paolini et al., 1994). This protein is the ligand for CCR8, a receptor expressed by Th2-lymphocytes, which can also be activated by vMIP-II (Sozzani et al., 1998). Thus, while the amino terminal domain of CC chemokines have been implicated in self-association and engagement of cognate receptors, vMIP-II lacks an effective dimer interface, potentially resulting in increased exposure of residues that are available to solvent in this region. This provides a potential mechanism for the ability of this virally encoded protein to bind to a broad spectrum of human chemokine receptors. The absence of self-association by vMIP-II may also be the basis for the ability of this virally encoded chemokine to stimulate signal transduction via CCR3 and CCR8, both of which bind chemokine ligands that exist in solution predominantly as monomers.

Comparison of vMIP-II to MIP-1β

The structure of vMIP-II provides several insights into the inability of this protein to form a dimer. Probably the most useful comparison with respect to dimerization is with MIP-1β, a CC chemokine that shares the most sequence identity (around 40%) to vMIP-II among chemokines of known structure (Fig. 1), has a very similar tertiary fold to vMIP-II (Lodi et al., 1994), and also tightly binds the chemokine receptor CCR5 (Combadiere et al., 1996; Raport et al., 1996; Samson et al., 1996). However, while MIP-1β activates CCR5, vMIP-II is an antagonist to CCR5 (Boshoff et al., 1997; Kledal et al., 1997).

The dimer of MIP-1β is comprised largely of hydrophobic interactions and involves many N-terminal residues that make contact with both the N-terminus of the other subunit and with several other non-N-terminal residues of the other subunit (Lodi et al., 1994). One important set of interactions in the MIP-1β dimer

involves the side chain of Phe13 in one subunit making extensive contact with both the Thr9′ and Leu34′ side chains of the other subunit. The significance of this contact is underscored by our preliminary result that a Phe13Ala mutation disrupts the ability of MIP-1β to dimerize (data not shown). A sequence alignment (Fig. 1) and a structural alignment of vMIP-II with MIP-1β reveals that vMIP-II does not possess appropriately positioned amino acids to make this crucial interaction. The equivalently positioned residues in vMIP-II are Leu16 (in place of Phe13 of MIP-1β), Asp12 (in place of Thr9), and Leu37 (same as Leu34). Figure 3A shows the MIP-1β dimer interface, while Figure 3B shows two vMIP-II monomers relatively positioned as a CC chemokine-type dimer, their positioning obtained by best fit superposition with the dimer of MIP-1β. As can be seen, the Phe13 of MIP-1β is Leu16 in vMIP-II, and this Leu16 does not have the wide, flat surface of a Phe that may be ideal for a fit into the putative hydrophobic pocket of the dimer that is formed in part by the Leu37′ (Leu34′ in MIP-1β). Perhaps more importantly, Thr9′ of MIP-1β is Asp12 in vMIP-II. This residue in MIP-1β interacts with Phe13 of the other subunit, completing the hydrophobic pocket formed by Phe13, Leu34′, and Thr9′. An Asp in place of Thr, as occurs in vMIP-II, cannot contribute to the formation of a hydrophobic pocket, and would not be expected to make favorable dimer contacts with the side chain of Leu16. In addition, when two vMIP-II monomers are aligned to make a CC chemokine-type dimer as shown in Figure 3B, this Asp12 becomes buried, an unfavorable situation that probably contributes significantly to the lack of ability of vMIP-II to dimerize.

Also possibly contributing to the lack of a dimer in vMIP-II is Lys13, which in MIP-1β is Ala10. In the MIP-1β dimer, this amino acid is near the symmetry point of the molecule and is expected to contact its counterpart in the other subunit. Even assuming that the two lysine side chains in vMIP-II avoid like-charge repulsions, the local structural changes required to accommodate the Lys13 of two subunits of vMIP-II rather than an alanine may alter the configuration in the area sufficiently to disrupt the hydrophobic contacts of a dimer.

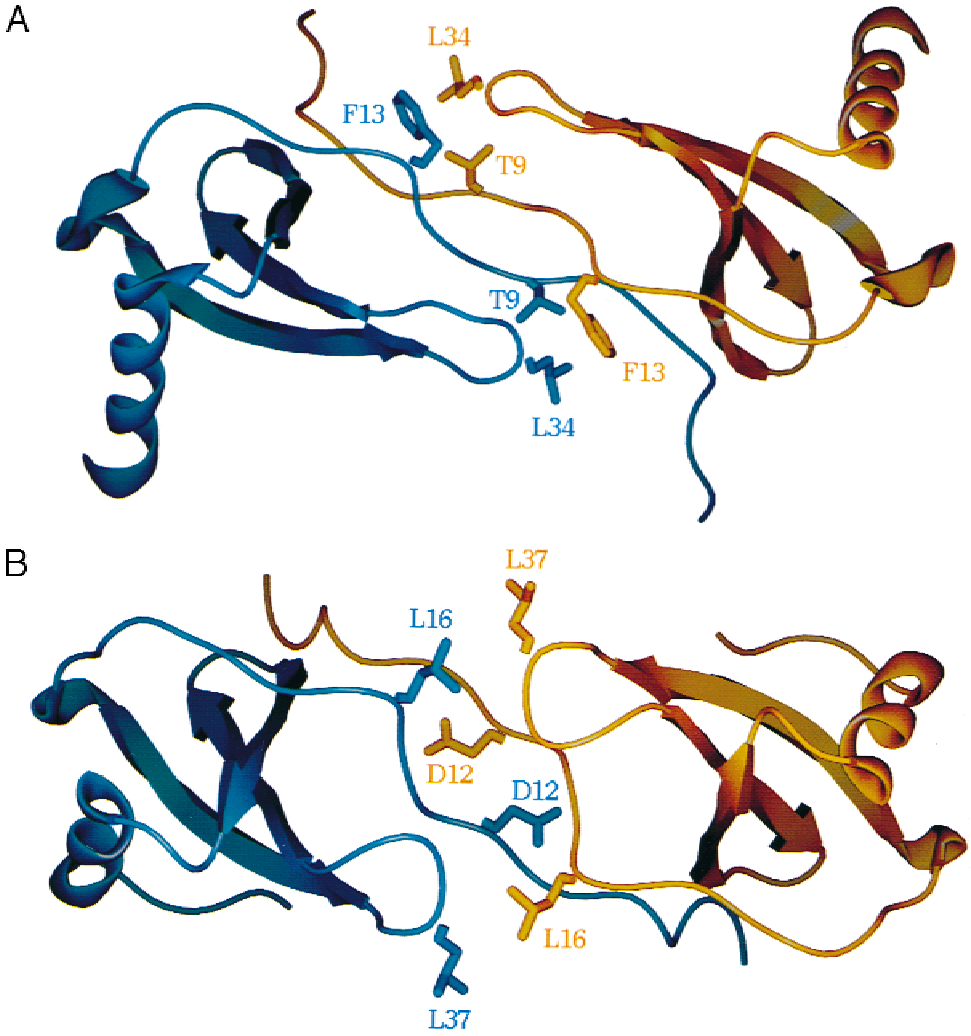

Fig. 3. A: A ribbon diagram of MIP-1β, showing the side chains for three residues at the dimer interface (Thr9, Phe13, Leu34). Structure obtained from reference (Lodi et al., 1994). PDB number: 1HUM. **B:** A ribbon diagram of two vMIP-II monomers, placed into the position of a MIP-1β-type dimer by superpositioning each vMIP-II monomer onto a subunit of the MIP-1β dimer (Lodi et al., 1994). The superpositioning was done for Cα atoms and the two proteins were matched over the three β-strands and the N-terminal region near the conserved cysteines. Figure 3 was created using the program SPOCK (Christopher, 1998).

Despite these specific differences between vMIP-II and MIP-1β, a comparison of their overall structure reveals them to be quite similar, with an RMSD of 1.6 Å upon best fitting the Cα over residues 14–56 for vMIP-II (11–53 for MIP-1β) and an RMSD of 0.83 Å when a best fit is performed on the three β-strand regions. The turns between the β-strands and the α-helix occur with similar angles and positioning for the two proteins, which leads to the possibility that the "scaffolding" of vMIP-II is competent to form a dimer, despite the lack of specific residues that allow dimer formation. In support of this hypothesis, we have produced a chimeric vMIP-II that contains the N-terminus of MIP-1β grafted onto the β-sheet and α-helix of vMIP-II and preliminarily find that this protein is in equilibrium between the monomer and dimer form (unpublished). The functional consequences of this mutation are currently being explored.

Comparison of vMIP-II to eotaxin and SDF-1

The repertoire of chemokine receptors bound by vMIP-II includes CCR3 and CXCR4, which have both been implicated as HIV-1 coreceptors. However, the engagement of CCR3 by vMIP-II results in signal transduction, whereas vMIP-II does not activate CXCR4 (Boshoff et al., 1997; Sozzani et al., 1998). Eotaxin and SDF-1 show exclusive binding to CCR3 and CXCR4, respectively, and thus represent important structural models for comparison to vMIP-II.

Eotaxin has about 36% sequence identity with vMIP-II, with the highest levels of identity in the β2 and β3 strands (Fig. 1). Both chemokines appear to exist predominantly as a monomer, although observation of a monomer–dimer equilibrium was reported in the case of eotaxin (Crump et al., 1998). Both have an unstructured N-terminal region, and aside from the canonical Cys–Cys motif, seven amino acids are shared in an N-terminal segment of 26 residues (24 in eotaxin): Ala6, Ser7, Pro11, Arg21, Pro24, Gln25, and Leu27. The β-strand regions of the two proteins can be overlaid with an RMSD (using C^{α}) of 0.64 Å, although the turn between the β2 and β3 strands is quite different (Crump et al., 1998). The C-terminal α-helix of eotaxin is almost an entire turn longer than in vMIP-II and is of similar length to the helix in MIP-1β (Lodi et al., 1994; Crump et al., 1998).

Three regions of vMIP-II are more similar in sequence to eotaxin than they are to MIP-1β. First, near the N-terminus of the proteins, vMIP-II shares little or no identity with MIP-1β for the first seven amino acids, while both vMIP-II and eotaxin have an identical Ala–Ser pair. Due to the high degree of disorder in this part of the structures of all chemokines, it is difficult to assess the significance of these amino acids, although the N-terminus of chemokines has been shown to be crucially important to chemokine activity (Gong & Clark-Lewis, 1995; Gong et al., 1996; Weber et al., 1996; Wells et al., 1996; Pakianathan et al., 1997). The other regions of identity between vMIP-II and eotaxin that are not shared by MIP-1β are in the loop preceding the first β-strand (including the first amino acid in the strand), where both vMIP-II and eotaxin have an LeuXSer while MIP-1β has PheXVal; and in the region around the C-terminal α-helix, particularly Lys59 (vMIP-II)/Lys55 (eotaxin), where MIP-1β has Glu56. The difference in charge and reach at each of these positions may result in differential function due to a change in the ability to bind cell surface sugars or to naturally aggregate; although most chemokines have these abilities, their in vivo relevance is not yet known (Tanaka et al., 1993; Graham et al., 1994, 1996; Hoogewerf et al., 1997; Koopmann & Krangel, 1997). An additional similarity between vMIP-II and eotaxin is the disruption of their C-terminal α-helix by a proline, followed by several amino acids that have a largely extended conformation in solution (Crump et al., 1998). This structural feature is quite distinct from the α-helix of MIP-1β, which is as long as that of eotaxin, but which continues in a helical structure until the C-terminus of the protein (Lodi et al., 1994).

A structural understanding of the binding of vMIP-II to the chemokine receptor CXCR4 is difficult, due to the fairly extensive differences in sequence between this virally encoded chemokine and SDF-1, the exclusive natural ligand for this receptor (Fig. 1). This is particularly true in regions of SDF-1 that have been shown to be critical for high-affinity binding to CXCR4. It is of interest that vMIP-II binds CXCR4 at high affinity, yet it lacks the RFFESH motif that has been implicated as critical for engagement by SDF-1 (Crump et al., 1997). Although the overall folds of vMIP-II and SDF-1 are similar, they share only one identical amino acid prior to the first canonically conserved Cys (Ser7 in vMIP-II, Ser4 in SDF-1). Aside from the N-terminal region (which does have low similarity among chemokines), the overall identity between vMIP-II and SDF-1 is about 17%. The arrangement of secondary structural units and turns is largely the same, which may account for the ability of vMIP-II to bind to the same receptor as SDF-1. One difference between the structure of vMIP-II and SDF-1 is that the C-terminal α-helix of vMIP-II has a different angle with respect to the β-sheet than SDF-1, possibly due to variations in the packing of the hydrophobic core (Crump et al., 1997). In vMIP-II the α-helix is oriented more perpendicular (about 60°) to the β-sheet, while in SDF-1 the α-helix angle is more parallel (about 40°) (Crump et al., 1997; Dealwis et al., 1998). As to the question of why vMIP-II binds but does not activate through CXCR4, an explanation could range from the significant differences in sequence identity to the potential difference in quaternary structure, as SDF-1 has been reported to be a CXC chemokine-type dimer upon crystallization (Dealwis et al., 1998), although it is a monomer in solution (Crump et al., 1997). Indeed, the difficulty in verifying regions of chemokines that allow for their wide range of distinct activities is underscored by Crump et al. (1997), who constructed a series of mutants and chimeras of SDF-1. These workers found that many of the sequence and structural features of the protein that were predicted to be important for activity on the CXCR4 receptor were "paradoxically" not critical for binding or activation (Crump et al., 1997).

Conclusions

We have determined the solution structure of vMIP-II, a CC chemokine that is unique in its ability to cross-bind the receptors of both major chemokine subfamilies (CC and CXC), and whose binding ability imparts broad anti-HIV properties. Although vMIP-II has an overall fold that is similar to other known chemokines, this protein is fully monomeric and has significant sequence variation with other chemokines in several key regions, particularly at the N-terminus and at amino acid sites crucial for both CC and CXC dimer formation.

Materials and methods

Production and purification of vMIP-II

The gene for vMIP-II was generously provided by Dr. Patrick Moore and Dr. Yuan Chang, Columbia University. vMIP-II was

expressed in the Novagen (Milwaukee, Wisconsin) pET32a(+) expression vector, which allows production of the protein of interest along with a thioredoxin fusion tag. The vector containing the sequence encoding the mature form of vMIP-II was transformed into BL21(DE3), and an individual colony was grown in 1 L minimal medium containing $^{15}NH_4Cl$ (Martek Biosciences, Columbia, Maryland) as the only nitrogen source, and with either $^{13}C_6$-glucose (Martek Biosciences) or unlabeled glucose. Cells were induced at $A_{550} = 0.9$ by making the cell culture to 1 mM IPTG (Calbiochem, La Jolla, California) and harvested by centrifugation after 5 h (for the ^{15}N, ^{13}C preparation) or 4 h (for the ^{15}N preparations). The fusion protein was purified and cleaved as described previously (LiWang et al., 1999), except that in this case some fusion protein was also isolated from the cell supernatant by loading the crude supernatant directly onto a Ni chelating column. The protein was eluted with imidazole and dialyzed against 50 mM Tris pH8 and subsequently cleaved with enterokinase and purified as described (LiWang et al., 1999). The resulting protein begins with amino acids Leu4–Gly5–Ala6 (using the numbering system of our previous work; LiWang et al., 1999), which has been reported to be the mature N-terminus of vMIP-II (Kledal et al., 1997). Protein samples were lyophilized and the protein was dissolved in 10 mM sodium phosphate, 0.05% sodium azide (buffer pH 5.4), and the overall solution made to 5% D_2O for the "H_2O" samples. For the "D_2O" samples, the lyophilized protein was taken up in 10 mM NaOP, 0.025% sodium azide, buffer pH 5.0 (lower pH to correct for the effect of the D_2O), and an excess (about 5 mL) of 99% D_2O (Isotec, Miamisburg, Ohio) was added. The sample was relyophilized and the powder was dissolved in 99.996% D_2O (Isotec).

NMR spectroscopy

All spectra except ^{15}N relaxation measurements were recorded at 25 °C on a Varian UnityPlus 600 MHz spectrometer at Purdue University, equipped with a z-shielded gradient triple resonance probe. ^{15}N T_1 and T_2 measurements were collected at 25 °C on a Varian UnityPlus 500 MHz spectrometer at Texas A&M University in a manner identical to that described earlier (LiWang et al., 1999). Sample tubes were purchased from Shigemi Inc. (Allison Park, Pennsylvania). Chemical shift referencing is relative to DSS, using the method proposed by Wishart et al. (1995). Triple resonance spectra used to assign ^1H, ^{13}C, and ^{15}N resonances were acquired and processed as described earlier (LiWang et al., 1999). ^1H–^1H NOE distance restraints were obtained from ^{15}N- and ^{13}C-separated three- (LiWang et al., 1999) and four-dimensional NOESY spectra (Clore & Gronenborn, 1991, 1998; Bax & Grzesiek, 1993). $^3J_{HNH\alpha}$ values, determined from a three-dimensional HNHA spectrum (Vuister & Bax, 1993), were used as J coupling restraints during structure calculations with the program X-PLOR (Brünger, 1992). $^3J_{HNH\beta}$ and $^3J_{H\alpha H\beta}$ values, determined from three-dimensional HNHB (Archer et al., 1991; Madsen et al., 1993) and HACAHB-COSY spectra (Grzesiek et al., 1995), were used to determine the $\chi 1$ angles (60°, −60°, or 180°) of amino acid side chains. Further $\chi 1$ information for valine, isoleucine, and threonine residues were obtained from long-range J-coupling constants between backbone ^{15}N and $^{13}C'$ spins and side-chain methyl protons (Grzesiek et al., 1993; Vuister et al., 1993; Bax et al., 1994). $\chi 2$ Dihedral angle information for leucine residues was determined from three-bond ^{13}C–^{13}C J-couplings (Bax et al., 1992).

Structure calculations

Interproton distances were grouped into four ranges, depending on the corresponding NOESY cross-peak volume. Strong, medium, weak, and very weak cross-peaks were given distance ranges of 1.8–2.7 Å (1.8–2.9 Å for NOEs involving NH protons), 1.8–3.3 Å (1.8–3.5 Å for NOEs involving NH protons), 1.8–5.0 Å, and 1.8–6.0 Å (Bewley et al., 1998). Distances involving methyl groups were given an additional 0.5 Å for the upper bound. The program X-PLOR (Brünger, 1992) was used to calculated structures of vMIP-II using simulated annealing protocols (Nilges et al., 1991). In addition to the usual energy potentials for experimental distance and dihedral angle restraints, an energy potential for measured $^3J_{HNH\alpha}$ (Garrett et al., 1994) was applied as well. Also, a conformational database potential for nonbonded contacts was applied during all calculations (Kuszewski et al., 1996, 1997).

vMIP-II coordinates

The Protein Data Base accession number for the reported structure is 1vmp.

Acknowledgments

The authors would like to gratefully acknowledge Carol Post, Adam Zabell, John Kuszewski, John Marquardt, Marcel Ottiger, John Christopher, and James Sacchettini for helpful discussions; Marius Clore, Angela Gronenborn, John Kuszewski for software supplemental to X-PLOR; Frank Delaglio and Dan Garrett for NMR software; and James Sacchettini for use of his computers for some structure calculations. Funding was provided by an American Cancer Society Institutional Grant through the Purdue Cancer Center, and by the National Institutes of Health R01AI41346 and by NSF MCB9733907.

References

Alkhatib G, Combadiere C, Broder CC, Feng Y, Kennedy PE, Murphy PM, Berger EA. 1996. CC CKR5: A RANTES, MIP-1α, MIP-1β receptor as a fusion cofactor for macrophage-tropic HIV-1. *Science 272*:1955–1958.

Archer SJ, Ikura M, Torchia DA, Bax A. 1991. An alternative 3D NMR technique for correlating backbone ^{15}N with side chain Hβ resonances in larger proteins. *J Magn Reson 95*:636–641.

Baggiolini M. 1998. Chemokines and leukocyte traffic. *Nature 329*:565–568.

Baggiolini M, Dewald B, Moser B. 1997. Human chemokines: An update. *Annu Rev Immunol 15*:675–705.

Bax A, Grzesiek S. 1993. Methodological advances in protein NMR. *Acc Chem Res 26*:131–138.

Bax A, Max D, Zax D. 1992. Measurement of long-range ^{13}C-^{13}C *J* couplings in a 20-kDa protein–peptide complex. *J Am Chem Soc 114*:6923–6925.

Bax A, Vuister GW, Grzesiek S, Delaglio F, Wang AC, Tschudin R, Zhu G. 1994. Quantitative *J* correlation. *Methods Enzymol 239*:79–105.

Bazan JF, Bacon KB, Hardiman G, Wang W, Soo K, Rossi D, Greaves DR, Zlotnik A, Schall TJ. 1997. A new class of membrane-bound chemokine with a CX3C motif. *Nature 385*:640–644.

Bewley CA, Gustafson KR, Boyd MR, Covell DG, Bax A, Clore MG, Gronenborn AM. 1998. Solution structure of cyanovirin-N, a potent HIV-inactivating protein. *Nat Struct Biol 5*:571–578.

Bleul CC, Farzan M, Choe H, Parolin C, Clark-Lewis I, Sodroski J, Springer TA. 1996. The lymphocyte chemoattractant SDF-1 is a ligand for LESTR/fusin and blocks HIV-1 entry. *Nature 382*:829–833.

Boshoff C, Endo Y, Collins PD, Takeuchi Y, Reeves JD, Schweickart VL, Siani MA, Sasaki T, Williams TJ, Gray PW, Moore PS, et al. 1997. Angiogenic and HIV-inhibitory functions of KSHV-encoded chemokines. *Science 278*:290–294.

Brünger AT. 1992. *X-PLOR version 3.1: A system for X-ray crystallography and NMR*. New Haven, Connecticut: Yale University Press.

Burrows SD, Doyle ML, Murphy KP, Franklin SG, White JR, Brooks I, McNulty DE, Scott MO, Knutson JR, Porter D, et al. 1994. Determination of the monomer-dimer equilibrium of interleukin-8 reveals it is a monomer at physiological concentrations. *Biochemistry 33*:12741–12745.

Christopher JA. 1998. *SPOCK: The structural properties observation and calculation kit (Program Manual)*. College Station, Texas: Center for Macromolecular Design, Texas A&M University.

Chung C, Cooke RM, Proudfoot AEI, Wells TNC. 1995. The three-dimensional solution structure of RANTES. *Biochemistry 34*:3907–9314.

Clark-Lewis I, Kim K-S, Rajarathnam K, Gong J-H, Dewald B, Moser B, Baggiolini M, Sykes BD. 1995. Structure–activity relationships of chemokines. *J Leukoc Biol 57*:703–711.

Clore GM, Appella E, Yamada M, Matsushima K, Gronenborn AM. 1990. Three dimensional structure of interleukin-8 in solution. *Biochemistry 29*:1689–1696.

Clore GM, Gronenborn AM. 1991. Structures of larger proteins in solution: Three- and four-dimensional heteronuclear NMR spectroscopy. *Science 252*:1390–1399.

Clore GM, Gronenborn AM. 1998. Determining the structures of larger proteins and protein complexes by NMR. *Trends Biotechnol 16*:22–34.

Combadiere C, Ahuja SK, Tiffany HL, Murphy PM. 1996. Cloning and functional expression of CC CKR5, a human monocyte CC chemokine receptor selective for MIP-1α, MIP-1β, and RANTES. *J Leukoc Biol 60*:147–152.

Crump MP, Gong J-H, Loetscher P, Rajarathnam K, Amara A, Arenzana-Seisdedos F, Virelizier J-L, Baggiolini M, Sykes B, Clark-Lewis I. 1997. Solution structure and the basis for functional activity of stromal cell-derived factor-1; dissociation of CXCR4 activation from binding and inhibition of HIV-1. *EMBO J 16*:6996–7007.

Crump MP, Rajarathnam K, Kim K-S, Clark-Lewis I, Sykes BD. 1998. Solution structure of eotaxin, a chemokine that selectively recruits eosinophils in allergic inflammation. *J Biol Chem 273*:22471–22479.

Dealwis C, Fernandez EJ, Thompson DA, Simon RJ, Siani MA, Lolis E. 1998. Crystal structure of chemically synthesized [N33A]SDF-1a, a potent ligand for the HIV-1 "Fusin" co-receptor. *Proc Natl Acad Sci USA 95*:6941–6946.

Deng H, Liu R, Ellmeier W, Choe S, Unutmaz D, Burkhart M, Di Marzio P, Marmon S, Sutton RE, Hill CM, et al. 1996. Identification of a major co-receptor for primary isolates of HIV-1. *Nature 381*:661–666.

Doms RW, Peiper SC. 1997. Unwelcome guests with master keys: How HIV uses chemokine receptors for cellular entry. *Virology 235*:179–190.

Dragic T, Litwin V, Allaway GP, Martin SR, Huang Y, Nagashima KA, Cayanan C, Maddon PJ, Koup RA, Moore JP, Paxton WA. 1996. HIV-1 entry into CD4+ cells is mediated by the chemokine receptor CC-CKR-5. *Nature 381*:667–673.

Fairbrother WJ, Reilly D, Colby TJ, Hesselgesser J, Horuk R. 1994. The solution structure of melanoma growth stimulating activity. *J Mol Biol 242*: 252–270.

Farrow NA, Muhandiram R, Singer AU, Pascal SM, Kay CM, Gish G, Shoelson SE, Pawson T, Forman-Kay JD, Kay LE. 1994. Backbone dynamics of a free and a phosphopeptide-complexed Src homology 2 domain by 15N NMR relaxation. *Biochemistry 33*:5984–6003.

Garrett DS, Lodi PJ, Shamoo Y, Williams KR, Clore GM, Gronenborn AM. 1994. The impact of direct refinement against three-bond HN-C$^{\alpha}$H coupling constants on protein structure determination by NMR. *J Magn Reson Ser B 104*:99–103.

Gong J-H, Clark-Lewis I. 1995. Antagonists of monocyte chemoattractant protein 1 identified by modification of functionally critical NH_2-terminal residues. *J Exp Med 181*:631–640.

Gong J-H, Uguccioni M, Dewald B, Baggiolini M, Clark-Lewis I. 1996. RANTES and MCP-3 antagonists bind multiple chemokine receptors. *J Biol Chem 271*:10521–10527.

Graham GJ, MacKenzie J, Lowe S, Tsang L-S, Weatherbee JA, Issacson A, Medicherla J, Fang F, Wilkinson PC, Pragnell IB. 1994. Aggregation of the chemokine MIP-1α is a dynamic and reversible phenomenon. *J Biol Chem 269*:4974–4978.

Graham GJ, Wilkinson PC, Nibbs RJB, Lowe S, Kolset SO, Parker A, Freshney MG, Tsang ML-S, Pragnell IB. 1996. Uncoupling stem cell inhibition from monocyte chemoattraction in MIP-1a by mutagenesis of the proteoglycan binding site. *EMBO J 15*:6506–6515.

Grasberger BL, Gronenborn AM, Clore GM. 1993. Analysis of the backbone dynamics of interleukin-8 by ^{15}N relaxation measurements. *J Mol Biol 230*:364–372.

Grzesiek S, Kuboniwa H, Hinck AP, Bax A. 1995. Multiple-quantum line narrowing for measurement of H^{α}-H^{β} *J* couplings in isotopically enriched proteins. *J Am Chem Soc 117*:5312–5315.

Grzesiek S, Vuister GW, Bax A. 1993. A simple and sensitive experiment for measurement of J_{cc} couplings between backbone carbonyl and methyl carbons in isotopically enriched proteins. *J Biomol NMR 3*:487–493.

Hadley TJ, Peiper SC. 1997. From malaria to chemokine receptor: The emerging physiologic role of the Duffy blood group antigen. *Blood 89*: 3077–3091.

Handel TM, Domaille PJ. 1996. Heteronuclear (^{1}H, ^{13}C, ^{15}N) NMR assignments and solution structure of the monocyte chemoattractant protein-1 (MCP-1) dimer. *Biochemistry 35*:6569–6584.

Hanzawa H, Haruyama H, Konishi K, Watanabe K, Tsurufuji S. 1998. Solution structure of CINC/Gro investigated by heteronuclear NMR. *J Biochem 123*:62–70.

Holmes WE, Lee J, Kuang W-J, Rice GC, Wood WI. 1991. Structure and functional expression of a human interleukin-8 receptor. *Science 253*:1278–1280.

Hoogewerf AJ, Kuschert GSV, Proudfoot AEI, Borlat F, Clark-Lewis I, Power CA, Wells TNC. 1997. Glycosaminoglycans mediate cell surface oligomerization of chemokines. *Biochemistry 36*:13570–13578.

Kay LE, Torchia DA, Bax A. 1989. Backbone dynamics of proteins as studied by 15N inverse detected heteronuclear NMR spectroscopy: Application to staphylococcal nuclease. *Biochemistry 28*:8972–8979.

Kelner GS, Kennedy J, Bacon KB, Kleyensteuber S, Largaespada DA, Jenkins NA, Copeland NG, Bazan JF, Moore KW, Schall TJ, et al. 1994. Lymphotactin: A cytokine that represents a new class of chemokine. *Science 266*:1395–1399.

Kim K-S, Clark-Lewis I, Sykes BD. 1994. Solution structure of GRO/melanoma growth stimulatory activity determined by 1H NMR spectroscopy. *J Biol Chem 269*:32909–32915.

Kim K-S, Rajarathnam K, Clark-Lewis I, Sykes BD. 1996. Structural characterization of a monomeric chemokine: Monocyte chemoattractant protein-3. *FEBS Lett 395*:277–282.

Kledal TN, Rosenkilde MM, Coulin F, Simmons G, Johnsen AH, Alouani S, Power CA, Luttichau HR, Gerstoft J, Clapham PR, et al. 1997. A broad-spectrum chemokine antagonist encoded by Kaposi's Sarcoma-associated herpesvirus. *Science 277*:1656–1659.

Koopmann W, Krangel MS. 1997. Identification of a glycosaminoglycan-binding site in chemokine macrophage inflammatory protein-1α. *J Biol Chem 272*:10103–10109.

Kuboniwa H, Grzesiek S, Delaglio F, Bax A. 1994. Measurement of HN-Hα J couplings in calcium-free calmodulin using new 2D and 3D water-flip-back methods. *J Biomol NMR 4*:871–878.

Kuszewski J, Gronenborn AM, Clore GM. 1996. Improving the quality of NMR and crystallographic protein structures by means of a conformational database potential derived from structure databases. *Protein Sci 5*:1067–1080.

Kuszewski J, Gronenborn AM, Clore GM. 1997. Improvements and extensions in the conformational database potential for the refinement of NMR and X-ray structures of proteins and ucleic acids. *J Magn Reson 125*:171–177.

Kuszewski J, Nilges M, Brünger AT. 1992. Sampling and efficiency of metric matrix distance geometry: A novel "partial" matrix algorithm. *J Biomol NMR 2*:33–56.

Laskowski RA, MacArthur MW, Moss DS, Thornton JW. 1993. PROCHECK: A program to check to stereochemical quality of protein structures. *J Appl Crystallogr 26*:283–291.

Laurence JS, LiWang AC, LiWang PJ. 1998. The effect of N-terminal truncation and solution conditions on chemokine dimer stability: Nuclear magnetic resonance structural analysis of macrophage inflammatory protein 1β mutants. *Biochemistry 37*:9346–9354.

Leong SR, Lowman HB, Liu J, Shire S, Deforge LE, Gillece-Castro BL, McDowell R, Hébert CA. 1997. IL-8 single-chain homodimers and heterodimers: Interactions with the chemokine receptors CXCR1, CXCR2, and DARC. *Protein Sci 6*:609–617.

LiWang AC, Cao JJ, Zheng H, Lu Z, Peiper SC, LiWang PJ. 1999. Dynamics study on the anti-human immunodeficiency virus chemokine vrial macrophage inflammatory protein-II (vMIP-II) reveals a fully monomeric protein. *Biochemistry 38*:442–453.

Lodi PJ, Garrett DS, Kuszewski J, Tsang ML-S, Weatherbee JA, Leonard WJ, Gronenborn AM, Clore GM. 1994. High-resolution solution structure of the β chemokinehMIP-1β by multidimensional NMR. *Science 263*:1762–1767.

MacArthur MW, Thornton JM. 1991. Influence of proline residues on protein conformation. *J Mol Biol 218*:397–412.

Madsen JC, Sørensen OW, Sørensen P, Poulsen FM. 1993. Improved pulse sequences for measuring coupling constants in ^{13}C, ^{15}N-labeled proteins. *J Biomol NMR 3*:239–244.

Mayo K, Roongta V, Ilyina E, Milius R, Barker S. 1995. NMR solution structure of the 32-kDa platelet factor 4 ELR-motif N-terminal chimera: A symmetric tetramer. *Biochemistry 34*:11399–11409.

Meunier A, Bernassau J-M, Guillemot J-C, Ferrara P, Darbon H. 1997. Determination of the three-dimensional structure of CC chemokine monocyte chemoattractant protein 3 by ^{1}H two-dimensional NMR spectroscopy. *Biochemistry 36*:4412–4422.

Minor DL, Kim PS. 1994. Measurement of the β-sheet-forming propensities of amino acids. *Nature 367*:660–663.

Mizoue LS, Bazan JF, Johnson EC, Handel TM. 1999. Solution structure and dynamics of the CX3C chemokine domain of fractalkine and its interaction with an N-terminal fragment of CX3CR1. *Biochemistry 38*:1402–1414.

Moore PS, Boshoff C, Weiss RA, Chang Y. 1996. Molecular mimicry of human cytokine and cytokine response pathway genes by KSHV. *Science 274*:1739–1744.

Moser B, Dewald B, Barella L, Schumacher C, Baggiolini M, Clark-Lewis I. 1993. Interleukin-8 antagonists generated by N-terminal modification. *J Biol Chem 268*:7125–7128.

Murphy PM, Tiffany HL. 1991. Cloning and complementary DNa encoding a functional human interleukin-8 receptor. *Science 253*:1280–1283.

Neote K, DiGregorio D, Mak JY, Horuk R, Schall TJ. 1993. Molecular cloning, functional expression, and signalling characteristics of a C-C chemokine receptor. *Cell 72*:415–425.

Nilges M, Clore GM, Gronenborn AM. 1988. Determination of the three-dimensional structure of proteins from interproton distance data by hybrid distance geometry-dynamical simulated annealing calculations. *FEBS Lett 229*:317–324.

Nilges M, Kuszewski J, Brünger AT. 1991. In: Hoch JC, ed. *Computational aspects of the study of biological macromolecules by NMR*. New York: Plenum Press.

Oberlin E, Amara A, Bachelerie F, Bessia C, Virelizier J-L, Arenzana-Seisdedos F, Schwartz O, Heard J-M, Clark-Lewis I, Legler DF, et al. 1996. The CXC chemokine SDF-1 is the ligand for LESTR/fusin and prevents infection by T-cell-line-adapted HIV-1. *Nature 382*:833–835.

Oppenheim JJ, Zachariae COC, Mukaida N, Matsushima K. 1991. Properties of the novel proinflammatory supergene "intercrine" cytokine family. *Annu Rev Immunol 9*:617–648.

Paavola CD, Hemmerich S, Grunberger D, Polsky I, Bloom A, Freedman R, Mulkins M, Bhakta S, McCarley D, Wiesent L, et al. 1998. Monomeric monocyte chemoattractant protein-1 (MCP-1) binds and activates the MICP-1 receptor CCR2B. *J Biol Chem 273*:33157–33165.

Pakianathan DR, Kuta EG, Artis DR, Skelton NJ, Hebert CA. 1997. Distinct but overlapping epitopes for the interaction of a CC-chemokine with CCR1, CCR3, and CCR5. *Biochemistry 36*:9642–9648.

Paolini JF, Willard D, Consler T, Luther M, Krangel MS. 1994. The chemokines IL-8, monocyte chemoattractant protein-1, I-309 are monomers at physiologically relevant concentrations. *J Immunol 153*:2704–2717.

Rajarathnam K, Kay CM, Dewald B, Wolf M, Baggiolini M, Clark-Lewis I, Sykes BD. 1997. Neutrophil-activating peptide-2 and melanoma growth-stimulatory activity are functional as monomers for neutrophil activation. *J Biol Chem 272*:1725–1729.

Rajarathnam K, Sykes BD, Kay CM, Dewald B, Geiser T, Baggiolini M, Clark-Lewis I. 1994. Neutrophil activation by monomeric interleukin-8. *Science 264*:90-92.

Raport CJ, Gosling J, Schweickart VL, Gray PW, Charo IF. 1996. Molecular cloning and functional characterization of a novel human CC chemokine receptor (CCR5) for RANTES, MIP-1β, and MIP-1α. *J Biol Chem 271*:17161–17166.

Richardson JS. 1981. The anatomy and taxonomy of protein structure. *Adv Protein Chem 34*:167–339.

Rollins BJ. 1997. Chemokines. *Blood 90*:909–928.

Samson M, Labbe O, Mollereau C, Vassart G, Parmentier M. 1996. Molecular cloning and functional expression of a new human CC-chemokine receptor gene. *J Biol Chem 35*:3362–3367.

Schall TJ. 1991. Biology of the RANTES/SIS cytokine family. *Cytokine 3*:165–183.

Schraufstatter IU, Ma M, Oades ZG, Barritt DS, Cochrane CG. 1995. The role of Tyr13 and Lys15 of interleukin-8 in the high affinity interaction with the interleukin-8 receptor type A. *J Biol Chem 270*:10428–10431.

Shao W, Fernandez E, Wilken J, Thompson DA, Siani MA, West J, Lolis E, Schweitzer BI. 1998a. Accessibility of selenomethionine proteins by total chemical synthesis: Structural studies of human herpesvirus-8 MIP-II. *FEBS Lett 441*:77–82.

Shao W, Jerva LF, West J, Lolis E, Schweitzer BI. 1998b. Solution structure of murine macrophage inflammatory protein-2. *Biochemistry 37*:8303–8313.

Simmons G, Clapham PR, Picard L, Offord RE, Rosenkilde MM, Schwartz TW, Buser R, Wells TNC, Proudfoot AEI. 1997. Potent inhibition of HIV-1 infectivity in macrophages and lyphocytes by a novel CCR5 antagonist. *Science 276*:276–279.

Skelton NJ, Aspiras F, Ogez J, Schall TJ. 1995. Proton NMR assignments and solution conformation of RANTES, a chemokine of the C-C type. *Biochemistry 34*:5329–5342.

Sozzani S, Luini W, Bianchi G, Allavena P, Wells TNC, Napolitano M, Bernardini G, Vecchi A, D'Ambrosio D, Mazzeo D, et al. 1998. The viral chemokine macrophage inflammatory protein-II is a selective Th2 chemoattractant. *Blood 92*:4035–4039.

Tanaka Y, Adams DH, Hubscher S, Hirano H, Siebenlist U, Shaw S. 1993. T-cell adhesion induced by proteoglycan-immobilized cytokine MIP-1β. *Nature 361*:79–82.

Thompson JD, Higgins DG, Gibson TJ. 1994. CLUSTAL W: Improving the sensitivity of progressive multiple sequence alignment through sequence weighting. *Nucl Acids Res 22*:4673–4680.

Vuister GW, Bax A. 1993. Quantitative *J* correlation: A new approach for measuring homonuclear three-bond $J(\mathrm{HNH}\alpha)$ coupling constants in ^{15}N-enriched proteins. *J Am Chem Soc 115*:7772–7777.

Vuister GW, Wang AC, Bax A. 1993. Measurement of three-bond nitrogen-carbon *J* couplings in proteins uniformly enriched in ^{15}N and ^{13}C. *J Am Chem Soc 115*:5334–5335.

Wagner L, Yang OO, Garcia-Zepeda EA, Ge Y, Kalams SA, Walker BD, Pasternack MS, Luster AD. 1998. β-Chemokines are released from HIV-1 specific cytolytic T-cell granules complexed to proteoglycans. *Nature 391*:908–911.

Weber M, Uguccioni M, Baggiolini M, Clark-Lewis I, Dahinden CA. 1996. Deletion of the NH_2-terminal residue converts monocyte chemotactic protein 1 from an activator of basophil mediator release to an eosinophil chemoattractant. *J Exp Med 183*:681–685.

Wells TNC, Power CA, Lusti-Narasimhan M, Hoogewerf AJ, Cooke RM, Chung C, Peitsch MC, Proudfoot AEI. 1996. Selectivity and antagonism of chemokine receptors. *J Leukoc Biol 59*:53–60.

Wishart DS, Bigam CG, Yao J, Abildgaard F, Dyson HJ, Oldfield E, Markley JL, Sykes BD. 1995. ^{1}H, ^{13}C, ^{15}N chemical shift referencing in biomolecular NMR. *J Biomol NMR 6*:135–140.

Zhang X, Chen L, Bancroft DP, Lai CK, Maione TE. 1994. Crystal structure of human platelet factor 4. *Biochemistry 33*:8361–8366.

Zhang Y, Rollins BJ. 1995. A dominant negative inhibitor indicates that monocyte chemoattractant protein 1 functions as a dimer. *Mol Cell Biol 15*:4851–4855.